

Review

Complementary Powerful Techniques for Investigating the Interactions of Proteins with Porous TiO₂ and Its Hybrid Materials: A Tutorial Review

Yihui Dong ^{1,*}, Weifeng Lin ¹ , Aatto Laaksonen ^{2,3,4,5}  and Xiaoyan Ji ^{2,*}

¹ Department of Molecular Chemistry and Materials Science, Weizmann Institute of Science, Rehovot 76100, Israel; lin.weifeng@weizmann.ac.il

² Energy Engineering, Division of Energy Science, Luleå University of Technology, 97187 Luleå, Sweden; aatto.laaksonen@mmk.su.se

³ Arrhenius Laboratory, Department of Materials and Environmental Chemistry, Stockholm University, 10691 Stockholm, Sweden

⁴ Center of Advanced Research in Bionanoconjugates and Biopolymers, “Petru Poni” Institute of Macromolecular Chemistry, 700469 Iasi, Romania

⁵ State Key Laboratory of Materials-Oriented and Chemical Engineering, Nanjing Tech University, Nanjing 211816, China

* Correspondence: yihui.dong@weizmann.ac.il (Y.D.); xiaoyan.ji@ltu.se (X.J.)

Abstract: Understanding the adsorption and interaction between porous materials and protein is of great importance in biomedical and interface sciences. Among the studied porous materials, TiO₂ and its hybrid materials, featuring distinct, well-defined pore sizes, structural stability and excellent biocompatibility, are widely used. In this review, the use of four powerful, synergetic and complementary techniques to study protein-TiO₂-based porous materials interactions at different scales is summarized, including high-performance liquid chromatography (HPLC), atomic force microscopy (AFM), surface-enhanced Raman scattering (SERS), and Molecular Dynamics (MD) simulations. We expect that this review could be helpful in optimizing the commonly used techniques to characterize the interfacial behavior of protein on porous TiO₂ materials in different applications.

Keywords: porous materials; TiO₂; high-performance liquid chromatography (HPLC); atomic force microscopy (AFM); surface enhanced Raman scattering (SERS); molecular dynamics (MD) simulations



Citation: Dong, Y.; Lin, W.; Laaksonen, A.; Ji, X. Complementary Powerful Techniques for Investigating the Interactions of Proteins with Porous TiO₂ and Its Hybrid Materials: A Tutorial Review. *Membranes* **2022**, *12*, 415. <https://doi.org/10.3390/membranes12040415>

Academic Editor: Rahul Singh

Received: 23 March 2022

Accepted: 8 April 2022

Published: 11 April 2022

Publisher's Note: MDPI stays neutral with regard to jurisdictional claims in published maps and institutional affiliations.



Copyright: © 2022 by the authors. Licensee MDPI, Basel, Switzerland. This article is an open access article distributed under the terms and conditions of the Creative Commons Attribution (CC BY) license (<https://creativecommons.org/licenses/by/4.0/>).

1. Introduction

Proteins interacting with surfaces of various substrates play a pivotal role in bio-engineering and medicine and are of fundamental importance for developing new nanotechnologies and designing nanomaterials for biological applications [1]. Understanding the adsorption and interactions between porous materials and biosystems is critical in environmental and biomedical sciences. One of the most investigated porous materials, TiO₂, has been extensively used in many industrially relevant applications ranging from environment to life sciences due to its efficient photoactivity, high chemical/thermal stability, and low cost [2]. Although TiO₂ has been intensively studied in various fields, using TiO₂ in bio-related applications is much more attractive [3]. This is because TiO₂ is a favorable biomaterial for manipulating biomolecules due to its excellent biocompatibility [3], controllable structural properties (morphology, crystal form, chemistry), as well as its long-term stability compared to other widely-used materials (i.e., porous silica [4], nanoporous sol-gel arrays [5]). The first studies were reported in the 1990s owing to the use of titanium in implants and the need to understand the interaction of biomolecules with implant surfaces covered with oxidized titanium [6,7]. Soon afterwards, this field developed quite quickly, and the number of publications began to exponentially increase. TiO₂ interacting with

biomolecules establishes a series of nanoparticle/biological interfaces, and their properties and process performance depend on a combination of different physicochemical interactions. Probing and determining these various interfacial interactions allows the development of predictive relationships between structure and properties/performance.

When these porous materials were introduced to the biological field, controlling the interaction between porous materials and biomolecules became a challenging problem for different applications, such as bio-separation, biosensors, drug delivery, and bio-detection [1,8]. It is widely accepted and recognized that the adsorption capacity of proteins provides a general criterion for determining the interaction strength between the protein and the adsorbed surfaces [9–12]. The widely and directly used approaches to control the interactions is through controlling the adsorption capacity. However, the adsorption capacity alone is not always a good indicator of interaction strength because the adsorption amount does not always correctly reflect effective protein surface attachment. More in-depth understanding and characterizations of the interactions between proteins and porous materials are needed for investigating interfacial interactions.

It is well-known that the performance of proteins separation/purification using chromatography mainly relies on regulating the protein interaction with related surfaces. The retention behavior test by chromatography can qualitatively represent the interaction strength between the protein and the solid surfaces. Thus, high performance liquid chromatography (HPLC) has been used as a reliable technique to study the interaction strength of proteins with the column materials at the macroscale [13]. However, the chromatographic retention time is unable to provide the information on molecular interactions at the nanoscale [14,15], and alternative options are needed to determine the interactions at the nano/microscale.

Atomic Force Microscopy (AFM), which possesses sensitivity at the nanoscale, can achieve molecular resolution of adsorbed molecules and directly reflect the atomic/molecular-level interactions [16]. This technique has undoubtedly made a considerable impact on life sciences in characterizing and manipulating biological interfaces [16,17], and provides both quantitative and dynamic information about protein interaction at the nanoscale [18,19]. Many studies have been conducted on evaluating protein interactions on a biomaterial surface [20–25]. The AFM-measured interaction force is related to the effective contact area between the AFM-tip and the related surfaces [26]. Depending on the number of protein molecules immobilized on the tip, it is a challenge to obtain the effective number of protein molecules in direct contact with the surface. Thus, exploring an efficient way to quantify the AFM-measured interaction force is of great importance.

Raman is another advanced and largely used technique for the structural characterization of molecules by analyzing their vibrational transition spectra, which has penetrated to applications in electrochemistry, catalysis, biology, materials science, and others [27–29]. To further improve the sensitivity, surface-enhanced Raman scattering (SERS) has been developed and recognized as a sensitive analysis technique that features significantly amplified Raman signals, enabling even single-molecule detection [30]. SERS is also a powerful technique for obtaining the orientation and interaction of adsorbed protein on the active-substrates through measuring the vibrational spectra of protein molecules adsorbed on the surface [27,31]. Regulation of SERS active-substrates is often used to improve the sensitivity and selectivity for bio-detection [30], especially for the semiconductor-based materials used as SERS active-substrates [32–35] with a low SERS intensity, for instance, structural optimization, modification and composition. Meanwhile, adjusting the experimental conditions, including pH values [36,37], temperature [38,39], and ionic strength [40,41], is often used to regulate the interaction strength of the adsorbed proteins [42], leading to a significant increase in sensitivity [43]. Thus, developing different ways to improve the semiconductor-based SERS is crucial.

To gain a more quantitative description and understanding of the protein interactions with solid-surfaces at the molecular level, theoretical studies and simulations can be used for estimations [15,44–47]. MD simulations are an important tool for exploring the atomistic

mechanisms involved in the adsorption process in complex biological systems [48]. In particular, it offers a method to analyze the synergic effects of surface nanomorphology and chemical compositions on the adsorption dynamics of proteins on nanostructured substrates [49]. Furthermore, the MD simulations can be applied to predict the adsorptive behavior and orientation of proteins, which provides a fundamental understanding at the molecular level.

In this review, the research on using these typical techniques to study the protein-TiO₂-based porous material interactions at different scales was summarized and the scenarios and scales where the interfacial phenomena play a key role were focused on. The main techniques include high-performance liquid chromatography (HPLC) at macroscale, atomic force microscopy (AFM) at mesoscale, surface enhanced Raman scattering (SERS) at nanoscale, and molecular simulation (MD) at nanoscale. We intend to discuss different techniques for understanding the protein interaction with the widely-used TiO₂-based materials.

2. Materials and Methods

2.1. HPLC-Based Techniques on Biomolecule-TiO₂ Interactions

The separation and purification of proteins are important for DNA sequencing, disease surveillance, and biopharmaceutical analysis [50–54], which mainly relies on the different interaction strengths of each protein with solid surfaces. An improved understanding of the protein–surface interaction is critical for predicting and controlling chromatographic separations [55–57]. The columns of HPLC are usually packed with the materials of pellicular or porous particles. The pellicular particles are made of polymer or glass beads surrounded by a thin, uniform layer of silica, alumina, polystyrene-divinyl-benzene synthetic or other types of ion-exchange resins. Nawrocki et al. had published a comprehensive review as a general guide to metal oxide affinity chromatography, including a description of pH stability, particle preparation and surface properties, as well as chromatographic chemistry [58,59]. Due to its amphoteric nature, hydrolytic stability at extreme pH, higher isoelectric point (pI) value than silica, TiO₂ has been used as an alternative material for column packing in HPLC [60]. Engholm-Keller et al. summarized the development of TiO₂-based chromatographic strategies for separating different biomolecules from introducing small molecules over 20 years ago to proteomics applications in 2011 [61].

In 1990s, Kawahara et al. used TiO₂ as column packing materials in HPLC to separate biogenic substances for the first time, revealing a high resistance of TiO₂ to both alkaline and acidic eluents [62]. These porous TiO₂ microspheres did further exhibit an excellent stability under high pressure and a variety of pH conditions, making them very suitable for HPLC applications. Chemie et al. compared the TiO₂ sorbent for HPLC with silica, alumina, and zirconia sorbent concerning its physical and chemical properties, finding that the TiO₂ sorbent enabled the separation of non-basic isomeric substance mixtures due to the Ti-OH groups on its surface [63]. Mazanek et al. chose TiO₂ as a chemo-affinity solid phase in HPLC for the selective enrichment of phosphopeptides [64]. Wijeratne et al. used the TiO₂ nanotubes grown radially on titanium wires and the commercial beads to separate phosphopeptides produced from complex tissue extracts of mouse liver [65]. The results showed that the TiO₂ nanotubes provide comparable efficacy for the enrichment of phosphopeptides and have the potential to be a low-cost and practical material in biological studies.

The structure of the material (surface area, pore size, etc.) is of great significance for the design of anti-fouling surfaces, chromatographic separation, and immobilized enzyme materials [6,8]. An et al. synthesized a new mesoporous TiO₂ and prepared it as the home-made chromatographic column to study the retention behavior of different proteins [66]. Inspired by the phenomenon that different surface structures can significantly affect protein adsorptive behavior, they also demonstrated that the different pore size of TiO₂ did alter the protein–surface interactions. They established a linearly predictive model between the geometry structure of TiO₂ and protein adsorption (Figure 1a), and combined the chromatographic retention behavior with this model (Figure 1b). In this predictive

model, the adsorption amount of proteins is translated into 1-dimensional interaction by squared root processing. Meanwhile, the geometrical parameters are combined due to the possibility of protein molecules contacting the TiO₂ surface by cubic root processing. The HPLC findings further verified and demonstrated the accuracy of the predictive adsorption model. The results showed that the affinity for the different proteins onto TiO₂ surfaces follows the order: lysozyme > BSA > myoglobin.

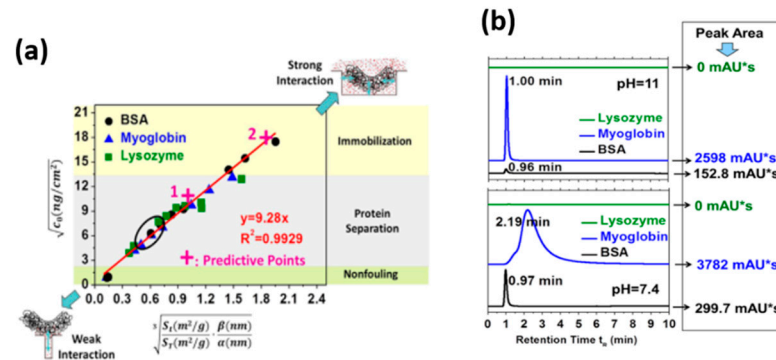


Figure 1. (a) A linearly predictive model between the geometry structure of mesoporous TiO₂ and protein adsorptive behavior. (b) HPLC measurements of each protein samples after passing through the imprinted home-made TiO₂ column. Reprinted from Ref. [66] with permission from Elsevier.

Dong et al. examined the interaction strength of protein with mesoporous TiO₂ at the macroscale under different pH conditions with the HPLC measurements. They also investigated the effect of pH conditions on the molecular force of the protein molecule with TiO₂ to guide the HPLC measurements [42]. They found that the molecular force was related to the effective contact area of the charged protein molecule (Figure 2A), which further can be used directly to design the HPLC measurements by tuning the retention behavior of the protein under different pH conditions (Figure 2B), indicating that the retention behavior at the macroscale is related to the molecular force at the nanoscale and the larger the molecular force, the longer the retention time. Furthermore, they also studied the contributions of ionic strength on the protein–surface interaction, as well as the effects on the retention behaviors of the proteins tested by HPLC [67]. They found that the interaction between protein and TiO₂ became weaker when the ionic strength is high, and the retention behavior of the proteins by HPLC can be effectively detected under high ionic strength, corresponding to the shorter retention time and larger peak area.

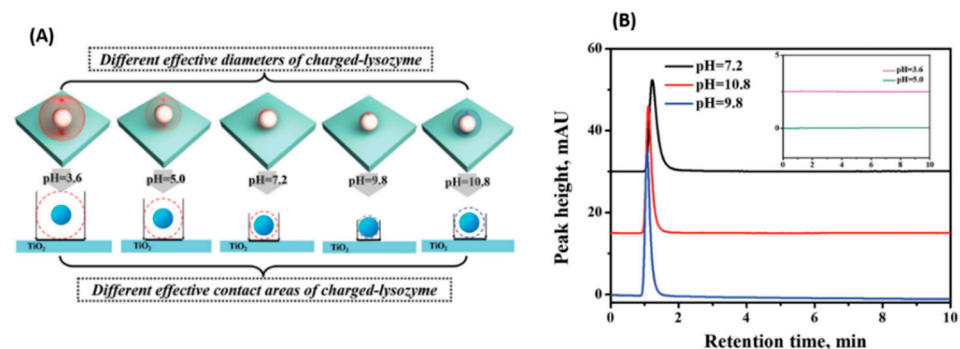


Figure 2. (A) Schematic diagram of the effective diameter of charged lysozyme, and the effective contact area of charged lysozyme with TiO₂ under different pH conditions. (B) HPLC retention behavior of lysozyme under different pH conditions passing through the imprinted home-made TiO₂ column. Reprinted from Ref. [42] with permission from Wiley.

More and more TiO₂-based hybrid materials have been widely used as chromatographic packing materials. Kupcik et al. reported using the amorphous TiO₂ nanotubes

(TiO₂NTs) and the corresponding hybrid materials decorated with Fe₃O₄ nanoparticles (TiO₂NTs@Fe₃O₄NPs) to achieve highly selective phosphopeptide enrichment [68]. Compared to those well-established TiO₂ microsphere materials, the enrichment efficiency and selectivity of TiO₂NTs and TiO₂NTs@Fe₃O₄NPs for phosphopeptides were increased to 28.7% and 25.3%, respectively. It indicated that both TiO₂NTs and TiO₂NTs@Fe₃O₄NPs provided good physicochemical properties which are favorable for highly selective phosphopeptide enrichment. Shen et al. used the titania-coated silica core–shell hybrid composites (TiO₂/SiO₂) as adsorbent, and combined with a liquid chromatography–tandem mass spectrometry for extraction and quantification of phospholipids from shrimp waste [69]. Recently, Dong et al. used the choline-based amino acid ionic liquid (IL) as the trace additives and loaded on mesoporous TiO₂ surface physically for the separation of two highly similar proteins (size, molecular weight, pI), lysozyme and cytochrome c [70]. The hydration properties of the ionic liquids loaded on the TiO₂ surface increased as the pH increased from 5.0 to 9.8, further weakening the protein interaction strength with the TiO₂ substrates, especially for lysozyme. They also studied the retention behavior of the mixed proteins passing through the TiO₂ column using HPLC and found that the introduction of ionic liquids (ILs) can separate the two highly similar proteins effectively.

Thus, TiO₂-based materials have been introduced as a popular material for affinity chromatography of biomolecules, where the behavior of biomolecules interacting with TiO₂ materials can be adjusted effectively, and the scope of applications of TiO₂-based chromatography in separation of various biomolecules has continuously expanded and increased.

2.2. AFM-Based Techniques on Biomolecule-TiO₂ Interactions

Different to the techniques that determine the interactions at the macroscale, atomic force microscopy (AFM) has been used as an effective and popular tool to reveal the mechanisms and investigate the interactions at the molecular level. The interaction force is exploited to keep the distance between the tip and the sample as a constant [71]. The most important feature of AFM is its ability to image samples in liquids, which is important for biological studies. AFM can enable the imaging of biological interfaces from cellular to molecular scales, indicating that it can directly visualize adsorbed proteins on different surfaces. In addition to imaging the surfaces, AFM can be used to obtain the interaction force between the tip and the sample by measuring the tip perpendicular to the surface while obtaining the force-distance curves [72].

In 2000, Cacciafesta et al. studied the fibrinogen adsorption on the ultraflat TiO₂ surfaces with AFM at molecular resolution [73]. The results showed that the ultraflat TiO₂ surface allowed visualization at the molecular resolution of both individual fibrinogen molecules and aggregates, while inferring a stronger interaction between the protein and the TiO₂ surface. Sousa et al. used AFM to perform the roughness and imaging analyses before and after protein adsorption. As shown in Figure 3, the roughness results revealed that the TiO₂ surfaces exhibited a lower roughness in air than in water before protein adsorption, which is probably due to the effect of the previously reported formation of the gel-like TiO₂ with a hydrated layer, rather than dehydrated oxides. While after protein adsorption, the height and phase images differed in morphology and contrast from the images on the surface without protein adsorption, and the roughness values were similar in air and in water [74].

Li et al. prepared the laccase-immobilized bacterial cellulose/TiO₂ functionalized hybrid membrane, and the installation of both TiO₂ and the functionalized hybrid membrane were confirmed by AFM [75]. The results showed that the surface was completely covered with laccase after the immobilization of laccase on the oxidized bacterial cellulose/TiO₂. Since TiO₂ is hydrophilic and has a high surface area, laccase can be easily loaded onto its surface. Meanwhile, the immobilized laccase showed better pH, temperature stability and reusability.

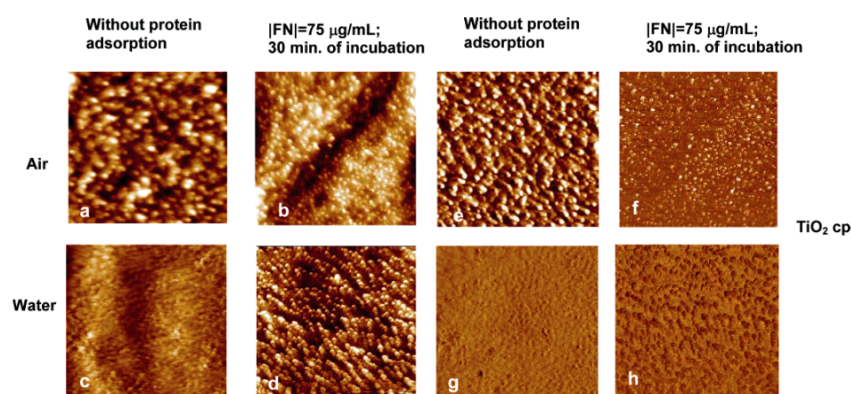


Figure 3. AFM height (a–d) and corresponding phase (e–h) images of TiO₂ recorded in air and water before and after protein adsorption. Reprinted from Ref. [74] with permission from American Chemistry Society.

A newly developed AFM-based single molecule force spectroscopy (SMFS) has been established as a reliable standard method to study single-molecule interactions [76–81]. Hoffmann and Dougan published a tutorial review about the SMF, and introduced two main operation modes for the force spectroscopy: force-extension and force-clamp [80]. They described the use of polyproteins to obtain clear mechanical fingerprints to monitor the protein response to applied mechanical forces [80]. Ganbaatar et al. performed the surface force analysis on TiO₂ with AFM by mounting a single amino acid residue on the AFM probe for the first time at the molecular level [82]. Force analysis on surfaces with three different crystal orientations revealed that the TiO₂ (110) surface has the unique property of adsorbing glycine molecules, showing different characteristics compared to the TiO₂ (001) and (100). Leader et al. used the single force spectroscopy to measure the adhesion forces between hydrophobic, aromatic and polar amino acids and TiO₂ surfaces. Compared with hydrophobic and uncharged amino acids, the aromatic and positively charged amino acids dominate in the affinity to the TiO₂ surface in this work [83].

AFM can be used to measure not only the conformational changes of proteins adsorbing on biomaterial surfaces, but also the interaction force between the proteins and the substrates by immobilizing the protein clusters onto the AFM tips according to the self-assembled monolayer (SAM) methods. Vergaro et al. investigated the interactions between human serum albumin (HSA) and different anatase TiO₂ nanoparticles, and found that the adhesion forces depended on the degree of hydrophilicity of the TiO₂ substrates. Surface roughness measurements showed that the molecules of HSA were arranged in a more globular manner on some of the nanocrystals. For nanocrystals with smaller primary particle size, lower protein affinity was found, which may correspond to their higher biocompatibility [84].

Although AFM can achieve a stretching of a single molecule or even measure a single bond [78,79], the results cannot reflect the overall effects of the solid surface at the nanoscale. This is because the solid surface, e.g., porous TiO₂, with different surface structures such as pore size and roughness, was utilized to control the protein interaction by adjusting the effective contact area between the protein and the substrate. This indicated that the AFM-measured interaction force is a total force which is related to the surface structure-induced contact area. How to obtain the molecular interaction of one single molecule with the solid surface decomposed from the interaction between the clusters and solid surface measured by AFM is of great interest but faces a difficult challenge. Dong et al. have created a series of works to quantify the molecular force of proteins with TiO₂ surfaces by combining the macroscopic experiment with microscopic measurements of AFM. In 2017, a new AFM-based approach was presented for the first time by Dong et al. to determine the molecular force between proteins and mesoporous TiO₂ with different surface roughness [85]. They reported that the molecular force was independent of the surface topography of the materials, as shown in Figure 4. Furthermore, they also extended the study to examine the effect of pH conditions

on the molecular force of protein molecule with TiO_2 using AFM [42]. They found that the molecular force is proportional to the pH-induced different effective diameter of charged protein, which is mainly due to the different corresponding effective contact area of one charged-protein molecule on the TiO_2 surface.

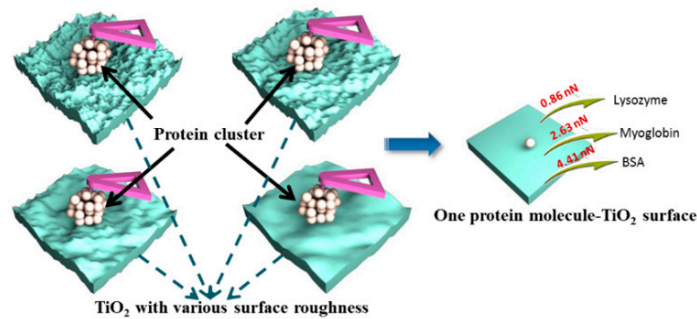


Figure 4. The molecular interaction of different proteins with TiO_2 with different surface roughness decomposed from the total adhesion force. Reprinted from Ref. [85] with permission from the American Chemistry Society.

To improve the conductivity of TiO_2 , surface modification to form hybrid TiO_2 –carbon materials has been an efficient strategy. These hybrid TiO_2 –carbon materials simultaneously possess both the electron conductivity of carbon and the corrosion resistance of TiO_2 materials. Dong et al. found that the molecular force of protein with TiO_2 measured by AFM can be enhanced by the heterogeneous carbon modification of the TiO_2 surface, as shown in Figure 5. The stronger interaction was due to the carbon modification being able to remove the $-\text{OH}$ on the TiO_2 surface, weaken the hydration ability, and further enhance the hydrophobicity of TiO_2 , leading to a stronger interaction with protein. The molecular force is independent of the surface roughness and structures but related to the chemistry of the C-TiO_2 , especially depending on the carbon coverages on the C-TiO_2 surface, and a carbon coverage of 58.3% achieves the largest molecular interaction force [86].

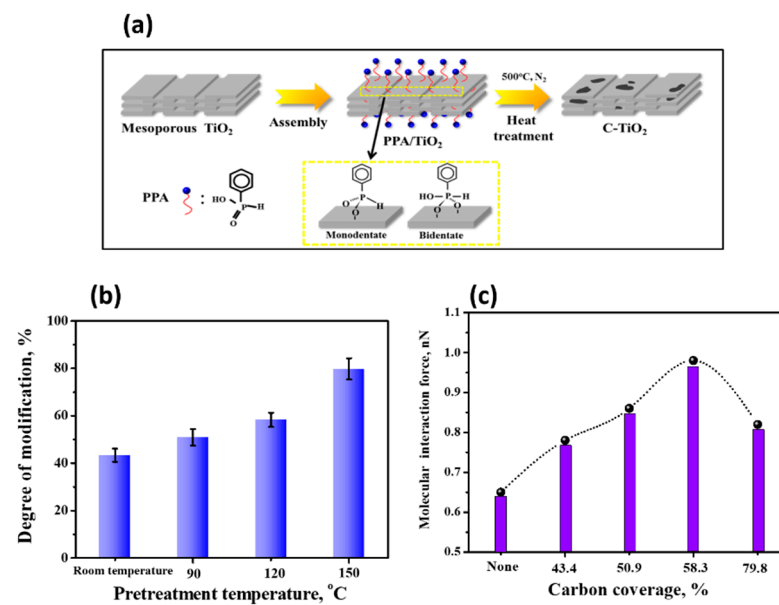


Figure 5. (a) Schematic diagram of the surface chemical modification of mesoporous TiO_2 to obtain C-TiO_2 ; (b) Different pretreatment temperatures corresponded to different carbon coverages of C-TiO_2 ; (c) The relationship between the molecular force of protein molecule with C-TiO_2 with different carbon coverages. Reprinted from Ref. [86] with permission from American Chemistry Society.

Besides the modification of the surface chemistry of TiO_2 , using additives to form composite TiO_2 substrate has been proposed as a desirable method to regulate the interactions between the adsorbed molecules and the related surfaces. Due to their unique physico-chemical properties, including high ionic conductivity, tunable chemical structures and stability, ionic liquids (ILs) have rapidly been widely-used in the field of biological analysis and protein chemistry. Meanwhile, due to their highly heterogeneous micro-compositions, ILs can change the microenvironment to adjust the interactions [87,88]. Based on this, Dong et al. loaded ionic liquid (IL) on the TiO_2 surface to investigate the protein interfacial interaction on the IL- TiO_2 hybrid materials [89]. By quantifying the AFM-based adhesion force, the molecular interaction forces of cytochrome c with TiO_2 and IL- TiO_2 surfaces were determined. The molecular forces of protein with TiO_2 for the systems, without IL, with IL in protein solution, and with ILs immobilized on the substrate, corresponded to the values of 1.65, 1.32, and 1.16 nN, respectively. It was shown that the molecular force was weakened after the addition of IL due to the hydration properties of the cation and anion of the IL.

The use of AFM has greatly advanced beyond high-resolution imaging to directly probe biomolecular interactions. Thus, AFM provides helpful insights into TiO_2 -based material design and protein- TiO_2 interactions toward biological applications at the molecular level. Especially, the molecular force between the protein and the TiO_2 -based material quantified by AFM through decomposing from the total adhesion forces are of great significance. Extending this method to quantify the molecular interaction force of other molecules is worth exploring.

2.3. SERS-Based Techniques on Biomolecule- TiO_2 Interactions

SERS spectroscopy is an effective and advanced technique for detecting biomolecules, owing to its high sensitivity to molecular structures, and is a nondestructive analysis method. In terms of signal intensity, the active substrate plays an important role in affecting the SERS performance. Semiconductors, i.e., TiO_2 , ZnO , and Fe_3O_4 , have been paid more and more attention to as SERS-active substrates, due to their superior properties, such as high stability, biocompatibility, and low cost [33,90–92]. A short review published by Cong et al. summarized the charge transfer transitions which are often the main contributors to the enhanced SERS activities in non-metal substrates, as shown in Figure 6 [93]. Based on the charge-transfer (CT)-induced SERS enhancement, a variety of semiconductor materials from inorganic to organic have been developed as novel SERS substrates [94].

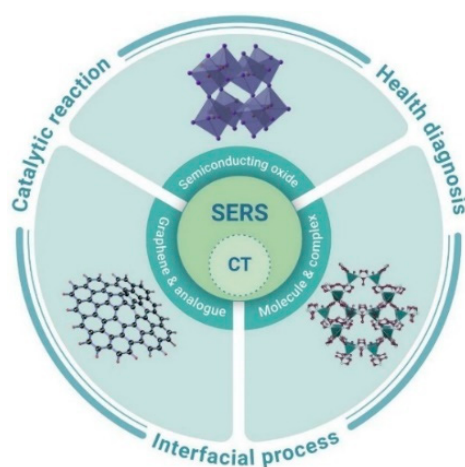


Figure 6. Schematic representing the charge-transfer (CT) induced SERS. The non-metal SERS substrates, including numerous types of semiconducting materials, such as semiconductor oxide, graphene and analogue, etc., were introduced with boosted SERS sensitivities. The promising applications include catalytic reaction, interfacial process, and health diagnosis, etc. Reprinted from Ref. [93] with permission from The Innovation.

Typically, as the most studied semiconductor materials, TiO₂-based materials have exhibited good SERS activity for detecting probe molecules [33,95–97]. Zhao et al. observed the SERS performance for the first time of the molecules adsorbed on the TiO₂ nanoparticles in 2008, which is attributed to the charge-transfer mechanism of TiO₂-to-molecule related to the surface state energy level of TiO₂ [96]. They also systematically investigated the effects of different crystallinity of TiO₂, pH conditions, and adsorption time on the SERS behavior and the interactions between adsorbed molecules and TiO₂ [97,98]. Subsequently, Musumeci et al. observed strong enhancement of biologically active enediol molecules adsorbed on TiO₂ nanoparticles with selected Raman active modes (Figure 7), and a molecule-to-TiO₂ charge-transfer mechanism was also proposed to explain this enhancement [33].

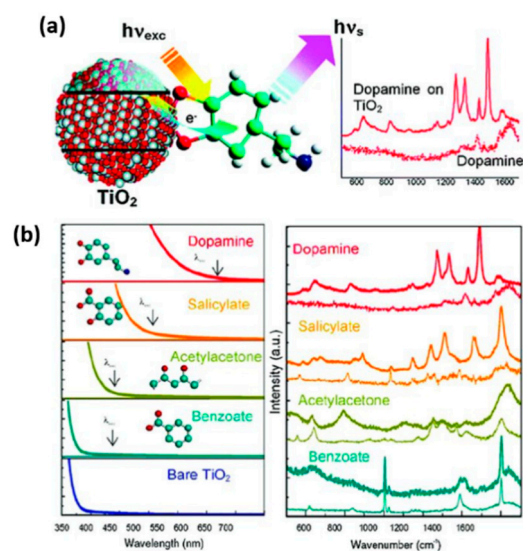


Figure 7. (a) Schematic illustration of SERS performance of dopamine adsorbed on TiO₂ nanoparticles. (b) Absorption and SERS spectra of TiO₂ nanoparticles modified with different ligands. Reprinted from Ref. [33] with permission from American Chemistry Society.

However, since TiO₂ is a low-conductivity semiconductor material, the detection sensitivity of TiO₂ materials for protein detection is low [99]. Thus, many works focused on using TiO₂ as a supporter of gold or silver to improve their SERS performances [100–103]. In addition to doping noble metals, the particle size, structure, surface defects, and optical band gap of substrates have been reported to have significant impacts on adjusting SERS performance [34,86,96–98,104,105]. Weidinger et al. prepared the TiO₂ electrodes with different nanostructures as a platform for SERS and electrochemistry [104]. The SERS performance is ascribed to the enhanced local electric field derived from the synergistic effect of adjacent TiO₂ nanorods. The results showed that the rougher surface could improve the SERS performance, and these nanostructured TiO₂ electrodes exhibited an excellent electric field enhancement, which was due to the high anisotropy of the TiO₂ nanostructure. Yang et al. observed that the SERS enhancements of probe molecules on TiO₂ nanoparticles with different phase structures exhibit different degrees. Moreover, the mixed crystal structure TiO₂ with a suitable ratio of rutile and anatase phase is favorable to SERS enhancement of molecules [97].

As a unique structure, TiO₂ nanotube arrays have attracted more and more attention and are used as a new kind of SERS-active substrate for protein detection, due to their intrinsically uniform structures, high stability, and electronic properties [100–103,106–109]. Öner et al. found that the TiO₂ nanotube electrodes can preserve the structural integrity and redox behavior, and then they used these TiO₂ nanotube electrodes with high biocompatibility and extraordinary spectroscopic properties to study the SERS performance of cytochrome b5 [108]. A strong SERS signal of the heme unit of cytochrome b5 was observed when the protein matrix was covalently immobilized to the TiO₂ nanotube electrode. The

higher SERS enhancement was attributed to the enhanced localized electric fields caused by the specific optical properties of the TiO₂ nanotubular geometry. Meanwhile, the SERS enhancements generally depend on the features of the substrates, especially the surface roughness. Dong et al. found that the rougher surface of TiO₂ substrates can adsorb more protein molecules and the SERS performance of Cyt c on TiO₂ nanotubes can correlate quantitatively with the surface roughness of the substrates [110]. Furthermore, the enhancement factor (EF) is often regarded as a key standard in SERS, while accurately obtaining EF in SERS is a long-term problem, and the main challenge is to obtain the amount of proteins effectively excited by the laser [111,112]. In this article, the values of EFs were successfully calculated by combing the AFM-measured adhesion force and the quantified molecular force, further revealing that the effective amount of adsorbed proteins contributed directly to the protein interaction with the related electrode surfaces, as shown in Figure 8.

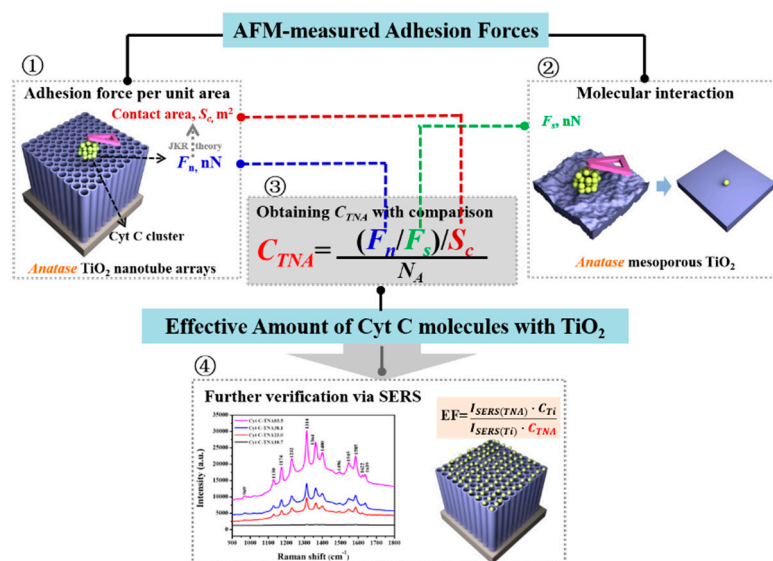


Figure 8. Scheme of the procedure for determining the effective amount of Cyt c molecules interacting with TiO₂ nanotube arrays (③) by AFM-measured adhesion forces (①) and molecular force (②), and further verification by SERS and the calculated EF (④). Reprinted from Ref. [110] with permission from Elsevier.

Recently, Dong et al. proposed an effective and new method to optimize the topography and structure of TiO₂ nanotube arrays through controlling the fluoride contents in the electrolyte. A significant enhancement of the SERS performance of Cyt c on these optimized TiO₂ nanotube arrays was obtained, demonstrating the importance of the structural integrity of the nanotubular on achieving excellent SERS performance in the trace detection of proteins, as shown in Figure 9 [113]. This is because the fluoride contents in the electrolyte can affect the sizes of cracks and the tube ruptures of TiO₂ nanotube arrays. It was found that the 0.2 wt % fluoride content can effectively provide the excellent and flat topography of TiO₂ nanotube arrays. Meanwhile, the results also showed that the interaction force between protein and TiO₂ nanotubes increased with decreasing the fluoride contents. They also found that the values of EF increased with the increase of the pore size of the TiO₂ nanotube arrays, which is generally a key factor affecting the SERS performance [114–117]. It indicated that the structure and topography can affect not only the properties of TiO₂ nanotubes, but also the interaction between the proteins and TiO₂.

Besides using the pure TiO₂ materials, Rajh et al. modified the semiconductors (e.g., TiO₂, Fe₃O₄, et al.) with enediol ligands and found that the intensity of the SERS enhancement depends on the electron density of the ligands, the number of surface binding sites, and the dipole moment. The SERS performance was observed for the bioconjugated system, and the potential was further investigated for the system in developing Raman-based

in vivo and vitro detection [118]. Zhao et al. prepared the TiO₂/ZnO semiconductor heterojunction and found that the charge-transfer efficiency and SERS performance can be significantly improved, where an EF of 10⁵ can be achieved for a non-resonance molecule with the lowest detection concentration down to 10⁻⁸ M [119]. Das et al. prepared porous Ag-TiO₂ film with nanocaged I structures as sensitive, recyclable, and low-cost SERS substrates to detect the various concentrations of blood urea for the first time. This new kind of porous Ag-TiO₂ film can be used as a level-free biosensor for the analysis of biomolecules in biological and clinical applications [120]. Dong et al. modified the TiO₂ with carbon to form the C-TiO₂ hybrid materials and observed an enhanced SERS performance of cytochrome c on these C-TiO₂ hybrid materials compared with the pure TiO₂ [86]. This is because the modification can form the graphene types of carbon, further leading to an enhanced SERS performance [121]. Furthermore, Dong et al. also chose the ionic liquids as trace additives to synthesize the ionic liquid-TiO₂ hybrid materials and used these hybrid materials as the active substrates to study the SERS performance of cytochrome c [87]. To the best of our knowledge, adding ionic liquids as additives into the SERS measurement to adjust the micro-environment has not been investigated before this work. The results showed that the determined EFs were 2.30×10^4 , 6.17×10^4 , and 1.19×10^5 , for the systems without ionic liquids, with ionic liquids in protein solutions and with ionic liquids immobilized on the substrate, respectively. These ionic liquid-TiO₂ hybrid materials allowed the obtaining of an exceptionally low detection limit even down to 10⁻⁹ M. The mechanism is due to the dissociation and hydration of ionic liquids occurring in the SERS system; the hydration properties of the ionic liquids result in an improved electron transfer ability of ionic liquids and further lead to an excellent SERS performance in protein detection [122,123]. This work stimulates the development of the use of ionic liquids in SERS and related applications in bioanalysis and nanoscience.

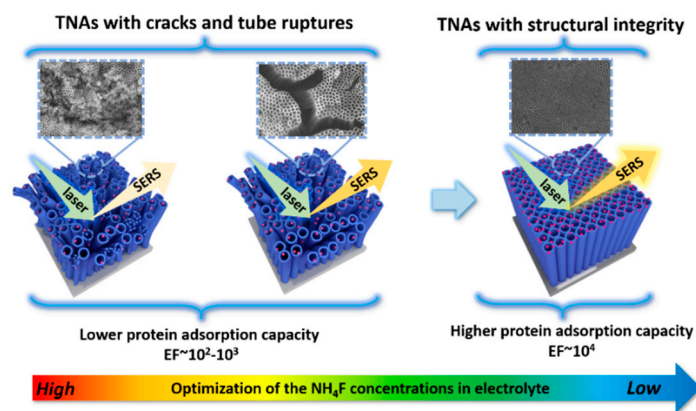


Figure 9. Schematic representation of SERS from Cyt c adsorbed on TiO₂ nanotube arrays with different structural integrities through optimization of the topography. Reprinted from Ref. [113] with permission from American Chemistry Society.

SERS is a highly selective, sensitive, and versatile technique to achieve fast data acquisition, showing considerable promise for qualitative and quantitative analysis for life science. Studying SERS performance of adsorbed proteins on TiO₂ meets the demands on trace detection in a variety of applications, also simulating the further development of TiO₂-based materials on trace detections.

2.4. Molecular Simulations

Experimental methods have been widely used to study the protein adsorptive behavior and interactions on a related surface, whereas molecular simulations are also well suited to provide insights into protein behavior on surfaces, i.e., orientation, conformation, and to providing molecular-level information [15,44,124]. A review of multiscale modeling and simulation methods for describing protein adsorption on surfaces with different properties

was presented by Quan et al. [125]. The water molecules at the interfaces play a key role in protein adsorption. Guo et al. found that a sufficient amount of interfacial hydration near the surface of nanostructured TiO₂ also promoted the attraction of fibronectin [126]. Kang et al. used molecular dynamics (MD) simulations to study the adsorption of human serum protein on non-hydroxylated and hydroxylated rutile TiO₂ surfaces [127]. Their results indicated that the distribution of interfacial water molecules caused by surface modification plays an important role in protein adsorption. The TiO₂ surface with the modification of hydroxyl groups was found to have a greater affinity to the protein, as shown in Figure 10. Zheng et al. studied the synergetic effects of hydroxylation state, surface nanostructure, and bioactive ions on the adsorption of collagen tripeptides to TiO₂ surfaces using molecular dynamics (MD) simulations [128]. They found that a dense water layer on the non-hydroxylated surface prevented tripeptide adsorption, but the water exhibited a less ordered and more dispersed distribution on the hydroxylated surfaces, which was suitable for adsorbing tripeptides.

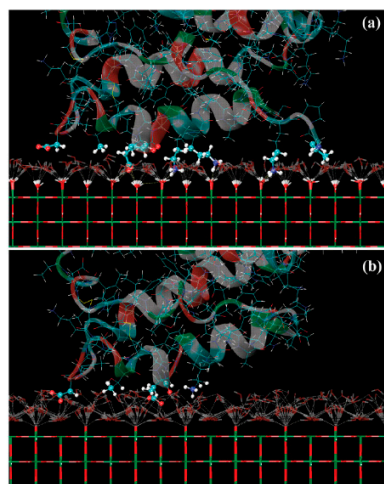


Figure 10. Snapshots of adsorption residues on (a) hydroxylated and (b) nonhydroxylated TiO₂ surfaces. Only the interfacial water molecules with the hydrogen bond network are shown and are displayed as white dashed lines. Reprinted from Ref. [127] with permission from American Chemistry Society.

Wu et al. studied the conformational dynamics of the fibronectin adsorbed on the rutile TiO₂ (110) surfaces by molecular dynamics (MD) simulations [129]. Their investigations showed that the binding strength and loss of protein secondary structure changed obviously, which depended on the surface topology of the substrate. Wu et al. also studied the binding of a negatively charged residue, aspartic acid, onto a negatively charged hydroxylated rutile TiO₂ (110) surface in an aqueous solution, containing monovalent cations by molecular dynamics (MD) simulations [130]. Their results indicated that ionic radii and charges would significantly affect adsorption geometry, hydration, and distance of cations from the rutile surface, further leading to the regulation of the Asp/rutile binding mode. Yang et al. investigated the orientation and conformation of myoglobin adsorbed on rutile TiO₂ (110) and (001) surfaces through the combination of the Monte Carlo and molecular dynamics (MD) methods [131]. Their simulation results showed that the adsorbed myoglobin conformations are not obviously affected by surfaces due to the strong hydrophilicity of both surfaces. However, the pathway of the electron transfer of myoglobin is closer to the rutile TiO₂ (001) surface, which is favorable for achieving the faster electron transfer (Figure 11).

Due to TiO₂ being easily contaminated by carboxylic acid (i.e., formate) in ambient environments, Wu et al. studied the different adsorptive behaviors of BSA on pure and formate-contaminated rutile TiO₂ (110) surface, respectively, for the first time [132]. They found that recontamination made further experimental studies difficult, despite numerous studies demonstrating that decontamination enhances albumin adsorption, which in

turn improves hemocompatibility on TiO₂ surfaces. Their MD simulation results showed that BSA could stably adsorb on the pure surface but the formate-contamination could decrease the TiO₂ surface polarity and then the adsorption of BSA (Figure 12). Furthermore, they controlled the surface wettability by imposing the formate contamination on the rutile TiO₂ (110) surface, and the adsorption properties of albumin and fibrinogen on the hydrophilic/hydrophobic TiO₂ surface were systematically investigated by MD simulations [133]. Their results found that the albumin is favorable to adsorb on the hydrophilic surface due to the albumin having a higher proportion of charged residues. However, the fibrinogen is favorable to adsorb on the hydrophobic surface due to the hydrophobic surface being able to help the fibrinogen diffuse to the surface and adjust its orientation to achieve stable adsorption.

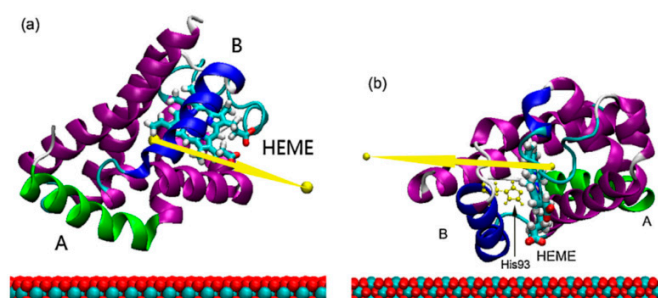


Figure 11. The adsorption configurations of myoglobin (a) on rutile TiO₂ (110) and (b) on rutile TiO₂ (001). The arrows represent the dipole direction of myoglobin. Reprinted from Ref. [131] with permission from Elsevier.

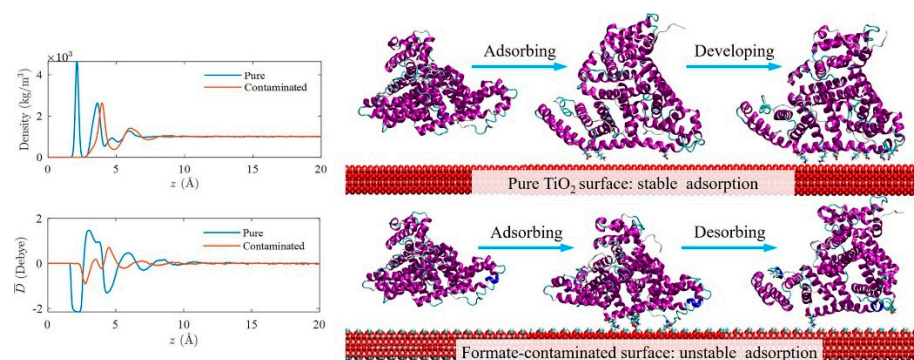


Figure 12. The density and dipole moment distributions of water molecules near the pure and formate contaminated surfaces; the scheme of the adsorption of BSA on pure TiO₂ and formate contaminated TiO₂ surface. Reprinted from Ref. [132] with permission from Elsevier.

MD simulation is a great tool which can provide many microscopic mechanisms and phenomena that cannot be observed directly in experiments. Especially for TiO₂-based materials, the simulation can provide detailed information on the effect of different crystal faces on the protein interaction, which behaves as a powerful tool to verify the interaction and clarify the mechanism at the molecular level.

3. Summary and Future Perspectives

In this review, different techniques for investigating the protein interaction with TiO₂-based materials are presented, including the HPLC retention behavior, atomic AFM-based topographies and interaction forces, SERS-induced detection performance, and MD simulations of orientation, conformation, and molecular-level information. Quantifying the molecular force between protein and TiO₂ under different realistic conditions (pH condition, surface structure and roughness, heterogeneity, etc.) is especially innovative, where the quantified molecular forces can be used as a guideline at the nanoscale to design

the experiments at the macroscale, such as HPLC-based protein separation, SERS-based protein bio-detection, and so forth. However, each technique is currently independent or qualitatively related due to the different scales studied. How to quantitatively correlate or combine these techniques at different scales is challenging. Researchers have also made many efforts to improve the combination of different techniques. For example, some in-situ techniques have been developed recently, such as Tip-Enhanced Raman Scattering (TERS) [134,135], which combines AFM and Raman with extremely high spatial resolution.

Moreover, the measured AFM-based interaction forces for the protein–solid surface systems can also be used to parameterize the force fields in molecular dynamics (MD) simulations. For such a complex interfacial system, MD simulations with all-atom force fields cannot fully grasp the interfacial properties, such as surface roughness and the adsorption of large amounts of proteins. The coarse-grained force field from AFM measurements could be an alternative for modeling the protein–solid interaction. Both the high precision AFM force measurement and the suitable model for a coarse-grained force field need to be advanced. Thus, it is expected that this review could be helpful for optimizing or combining these techniques for characterizing the interfacial behavior of protein on porous TiO₂ materials in different practical applications.

In addition to the techniques summarized in this review, some other techniques can also be used to investigate the interactions of protein–TiO₂ in the future. For example, Quartz crystal microbalance-dissipation (QCM-D), another advanced technique which enables real-time tracking of the adsorbed amount and viscoelastic properties of attached molecules at solid–liquid interfaces in biomolecular interaction processes [136–138]. Some optical techniques with the features of extremely high sensitivity have also been used to investigate the protein adsorptive behavior and trace detections, including ellipsometry, resonant waveguide gratings (RWG), surface plasmon resonance (SPR) [139], coupled plasmon-waveguide resonance spectroscopy (CPWR) [140], optical waveguide light-mode spectroscopy (OWLS) [141], and grating coupled interferometry (GCI) [142]. More and more advanced techniques are worth exploring to study the interactions between biomolecules and TiO₂-based materials.

Furthermore, for studying the protein interaction with hybrid TiO₂-based materials, introducing ionic liquids has been proved as an efficient method, i.e., ionic liquid-loaded TiO₂ on separating proteins and the addition of ionic liquid on TiO₂ on SERS detection. However, the analysis of the mechanisms still needs to be more in-depth. MD simulations could support understanding the mechanisms at the molecular level. Meanwhile, the classification of ionic liquids in the application of biological fields is also worth exploring. Furthermore, using different complementary methods to study more dynamic properties of protein with porous TiO₂-based materials, including frictional behavior, lubrication, drug delivery, and so forth, should be discussed in a simple tutorial type of summary.

Author Contributions: Y.D., writing—original draft. W.L., writing—review & editing. A.L., writing-review & editing. X.J., writing-review & editing, supervision. All authors have read and agreed to the published version of the manuscript.

Funding: This research received no external funding.

Institutional Review Board Statement: Not applicable.

Informed Consent Statement: Not applicable.

Data Availability Statement: Not applicable.

Acknowledgments: A. Laaksonen acknowledges the Swedish Research Council for financial support, and partial support from a grant from Ministry of Research and Innovation of Romania (CNCS-UEFISCDI, project number PN-III-P4-ID-PCCF-2016-0050, within PNCDI III). X. Ji thanks the financial support from the Swedish Research Council.

Conflicts of Interest: The authors declare no conflict of interest.

References

1. Nel, A.E.; Mädler, L.; Velegol, D.; Xia, T.; Hoek, E.M.V.; Somasundaran, P.; Klaessig, F.; Castranova, V.; Thompson, M. Understanding biophysicochemical interactions at the nano–bio interface. *Nat. Mater.* **2009**, *8*, 543–557. [[CrossRef](#)] [[PubMed](#)]
2. Chen, X.; Mao, S.S. Titanium dioxide nanomaterials: Synthesis, properties, modifications, and applications. *Chem. Rev.* **2007**, *107*, 2891–2959. [[CrossRef](#)] [[PubMed](#)]
3. Rajh, T.; Dimitrijevic, N.M.; Bissonnette, M.; Koritarov, T.; Konda, V. Titanium dioxide in the service of the biomedical revolution. *Chem. Rev.* **2014**, *114*, 10177–10216. [[CrossRef](#)] [[PubMed](#)]
4. Zhou, Z.; Hartmann, M. Progress in enzyme immobilization in ordered mesoporous materials and related applications. *Chem. Soc. Rev.* **2013**, *42*, 3894–3912. [[CrossRef](#)] [[PubMed](#)]
5. Park, S.-M.; Ahn, J.-Y.; Jo, M.; Lee, D.-K.; Lis, J.T.; Craighead, H.G.; Kim, S. Selection and elution of aptamers using nanoporous solgel arrays with integrated microheaters. *Lab Chip* **2009**, *9*, 1206–1212. [[CrossRef](#)] [[PubMed](#)]
6. Ellingsen, J.E. A study on the mechanism of protein adsorption to TiO₂. *Biomaterials* **1991**, *12*, 593–596. [[CrossRef](#)]
7. Martin, J.Y.; Schwartz, Z.; Hummert, T.W.; Schraub, D.M.; Simpson, J.; Lankford, J., Jr.; Dean, D.D.; Cochran, D.L.; Boyan, B.D. Effect of titanium surface roughness on proliferation, differentiation, and protein synthesis of human osteoblast-like cells (MG63). *J. Biomed. Mater. Res.* **1995**, *29*, 389–401. [[CrossRef](#)]
8. Limo, M.J.; Sola-Rabada, A.; Boix, E.; Thota, V.; Westcott, Z.C.; Puddu, V.; Perry, C.C. Interactions between Metal Oxides and Biomolecules: From Fundamental Understanding to Applications. *Chem. Rev.* **2018**, *118*, 11118–11193. [[CrossRef](#)]
9. Sang, L.-C.; Vinu, A.; Coppens, M.-O. General Description of the Adsorption of Proteins at Their Iso-electric Point in Na-noporous Materials. *Langmuir ACS J. Surf. Colloids* **2011**, *27*, 13828–13837. [[CrossRef](#)]
10. Zhuang, W.; Zhang, Y.; Zhu, J.; An, R.; Li, B.; Mu, L.; Ying, H.; Wu, J.; Zhou, J.; Chen, Y.; et al. Influences of geometrical topography and surface chemistry on the stable immobilization of adenosine deaminase on mesoporous TiO₂. *Chem. Eng. Sci.* **2016**, *139*, 142–151. [[CrossRef](#)]
11. Aramesh, M.; Shimoni, O.; Ostrikov, K.; Praver, S.; Cervenka, J. Surface charge effects in protein adsorption on nanodiamonds. *Nanoscale* **2015**, *7*, 5726–5736. [[CrossRef](#)] [[PubMed](#)]
12. Bayne, L.; Ulijn, R.V.; Halling, P.J. Effect of pore size on the performance of immobilised enzymes. *Chem. Soc. Rev.* **2013**, *42*, 9000–9010. [[CrossRef](#)] [[PubMed](#)]
13. Wang, F.; Min, Y.; Geng, X. Fast separations of intact proteins by liquid chromatography. *J. Sep. Sci.* **2012**, *35*, 3033–3045. [[CrossRef](#)] [[PubMed](#)]
14. Jung, S.; Abel, J.H.; Starger, J.L.; Yi, H. Porosity-Tuned Chitosan–Polyacrylamide Hydrogel Microspheres for Improved Protein Conjugation. *Biomacromolecules* **2016**, *17*, 2427–2436. [[CrossRef](#)]
15. Yu, G.; Liu, J.; Zhou, J. Mesoscopic coarse-grained simulations of hydrophobic charge induction chromatography (HCIC) for protein purification. *AIChE J.* **2015**, *61*, 2035–2047. [[CrossRef](#)]
16. Alsteens, D.; Gaub, H.E.; Newton, R.; Pfreundschuh, M.; Gerber, C.; Muller, D.J. Atomic force microscopy-based characterization and design of biointerfaces. *Nat. Rev. Mater.* **2017**, *2*, 17008. [[CrossRef](#)]
17. Cao, T.; Tang, H.; Liang, X.; Wang, A.; Auner, G.W.; Salley, S.O.; Ng, K.Y.S. Nanoscale investigation on adhesion of E. coli to surface modified silicone using atomic force microscopy. *Biotechnol. Bioeng.* **2006**, *94*, 167–176. [[CrossRef](#)]
18. Wang, M.S.; Palmer, L.B.; Schwartz, J.D.; Razatos, A. Evaluating Protein Attraction and Adhesion to Biomaterials with the Atomic Force Microscope. *Langmuir ACS J. Surf. Colloids* **2004**, *20*, 7753–7759. [[CrossRef](#)]
19. Tsapikouni, T.S.; Missirlis, Y.F. Protein-material interactions: From micro-to-nano scale. *Mater. Sci. Eng. B Adv. Funct. Solid State Mater.* **2008**, *152*, 2–7. [[CrossRef](#)]
20. Elter, P.; Lange, R.; Beck, U. Atomic force microscopy studies of the influence of convex and concave nanostructures on the adsorption of fibronectin. *Colloids Surf. B Biointerfaces* **2012**, *89*, 139–146. [[CrossRef](#)]
21. Tsapikouni, T.; Missirlis, Y.F. pH and ionic strength effect on single fibrinogen molecule adsorption on mica studied with AFM. *Colloids Surf. B Biointerfaces* **2007**, *57*, 89–96. [[CrossRef](#)] [[PubMed](#)]
22. Tencer, M.; Charbonneau, R.; Lahoud, N.; Berini, P. AFM study of BSA adlayers on Au stripes. *Appl. Surf. Sci.* **2007**, *253*, 9209–9214. [[CrossRef](#)]
23. Dupont-Gillain, C.C.; Fauroux, C.M.J.; Gardner, D.C.J.; Leggett, G.J. Use of AFM to probe the adsorption strength and time-dependent changes of albumin on self-assembled monolayers. *J. Biomed. Mater. Res. Part A* **2003**, *67*, 548–558. [[CrossRef](#)] [[PubMed](#)]
24. Xu, L.-C.; Logan, B.E. Interaction Forces Measured Using AFM between Colloids and Surfaces Coated with Both Dextran and Protein. *Langmuir ACS J. Surf. Colloids* **2006**, *22*, 4720–4727. [[CrossRef](#)]
25. Valle-Delgado, J.J.; Molina-Bolívar, J.A.; Galisteo-González, F.; Gálvez-Ruiz, M.J.; Feiler, A.; Rutland, M.W. Inter-action Forces between BSA Layers Adsorbed on Silica Surfaces Measured with an Atomic Force Microscope. *J. Phys. Chem. B* **2004**, *108*, 5365–5371. [[CrossRef](#)]
26. You, H.X.; Lowe, C.R. AFM studies of protein adsorption. 2. Characterization of immunoglobulin G adsorption by detergent washing. *J. Colloid Interface Sci.* **1996**, *182*, 586–601. [[CrossRef](#)]
27. Haldavnekar, R.; Venkatakrisnan, K.; Tan, B. Non plasmonic semiconductor quantum SERS probe as a pathway for in vitro cancer detection. *Nat. Commun.* **2018**, *9*, 3065. [[CrossRef](#)]

28. Tian, Z.Q. Surface-enhanced Raman spectroscopy: Advancements and applications. *J. Raman Spectrosc.* **2005**, *36*, 466–470. [[CrossRef](#)]
29. Palonpon, A.F.; Ando, J.; Yamakoshi, H.; Dodo, K.; Sodeoka, M.; Kawata, S.; Fujita, K. Raman and SERS microscopy for molecular imaging of live cells. *Nat. Protoc.* **2013**, *8*, 677–692. [[CrossRef](#)]
30. Langer, J.; de Aberasturi, J.D.; Aizpurua, J.; Alvarez-Puebla, R.A.; Auguie, B.; Baumberg, J.J.; Bazan, G.C.; Bell, S.E.J.; Boisen, A.; Brolo, A.G.; et al. Present and Future of Surface-Enhanced Raman Scattering. *ACS Nano* **2020**, *14*, 28–117. [[CrossRef](#)]
31. Yu, Q.; Golden, G. Probing the Protein Orientation on Charged Self-Assembled Monolayers on Gold Nanohole Arrays by SERS. *Langmuir ACS J. Surf. Colloids* **2007**, *23*, 8659–8662. [[CrossRef](#)] [[PubMed](#)]
32. Cecchini, M.P.; Turek, V.A.; Paget, J.; Kornyshev, A.A.; Edel, J. Self-assembled nanoparticle arrays for multiphase trace analyte detection. *Nat. Mater.* **2012**, *12*, 165–171. [[CrossRef](#)] [[PubMed](#)]
33. Musumeci, A.; Gosztola, D.; Schiller, T.; Dimitrijevic, N.M.; Mujica, V.; Martin, D.; Rajh, T. SERS of Semiconducting Nanoparticles (TiO₂ Hybrid Composites). *J. Am. Chem. Soc.* **2009**, *131*, 6040. [[CrossRef](#)]
34. Tarakeswar, P.; Finkelstein-Shapiro, D.; Hurst, S.J.; Rajh, T.; Mujica, V. Surface-Enhanced Raman Scattering on Semiconducting Oxide Nanoparticles: Oxide Nature, Size, Solvent, and pH Effects. *J. Phys. Chem. C* **2011**, *115*, 8994–9004. [[CrossRef](#)]
35. Schedin, F.; Lidorikis, E.; Lombardo, A.; Kravets, V.G.; Geim, A.K.; Grigorenko, A.N.; Novoselov, K.S.; Ferrari, A.C. Surface-Enhanced Raman Spectroscopy of Graphene. *ACS Nano* **2010**, *4*, 5617–5626. [[CrossRef](#)] [[PubMed](#)]
36. Liu, Y.; Yuan, H.; Fales, A.M.; Tuan, V.-D. pH-sensing nanostar probe using surface-enhanced Raman scattering (SERS): Theoretical and experimental studies. *J. Raman Spectrosc.* **2013**, *44*, 980–986. [[CrossRef](#)]
37. Kong, K.V.; Dinish, U.S.; Lau, W.K.O.; Olivo, M. Sensitive SERS-pH sensing in biological media using metal carbonyl functionalized planar substrates. *Biosens. Bioelectron.* **2014**, *54*, 135–140. [[CrossRef](#)]
38. Das, G.; Mecarini, F.; Gentile, F.; De Angelis, F.; Kumar, H.M.; Candeloro, P.; Liberale, C.; Cuda, G.; Di Fabrizio, E. Nano-patterned SERS substrate: Application for protein analysis vs. temperature. *Biosens. Bioelectron.* **2009**, *24*, 1693–1699. [[CrossRef](#)]
39. Yang, L.; Jiang, X.; Ruan, W.; Zhao, B.; Xu, W.; Lombardi, J.R. Adsorption study of 4-MBA on TiO₂ nanoparticles by surface-enhanced Raman spectroscopy. *J. Raman Spectrosc.* **2009**, *40*, 2004–2008. [[CrossRef](#)]
40. Erol, M.; Du, H.; Sukhishvili, S. Control of Specific Attachment of Proteins by Adsorption of Polymer Layers. *Langmuir ACS J. Surf. Colloids* **2006**, *22*, 11329–11336. [[CrossRef](#)]
41. Wang, J.; Anderson, W.; Li, J.; Lin, L.L.; Wang, Y.; Trau, M. A high-resolution study of in situ surface-enhanced Raman scattering nanotag behavior in biological systems. *J. Colloid Interface Sci.* **2019**, *537*, 536–546. [[CrossRef](#)] [[PubMed](#)]
42. Dong, Y.; Laaksonen, A.; Cao, W.; Ji, X.; Lu, X. AFM Study of pH-Dependent Adhesion of Single Protein to TiO₂ Surface. *Adv. Mater. Interfaces* **2019**, *6*, 1900411. [[CrossRef](#)]
43. Kang, H.; Haynes, C.L. Interactions between Silica-Coated Gold Nanorod Substrates and Hydrophobic Analytes in Colloidal Surface-Enhanced Raman Spectroscopy. *J. Phys. Chem. C* **2019**, *123*, 24685–24697. [[CrossRef](#)]
44. Zhou, J.; Chen, S.; Jiang, S. Orientation of Adsorbed Antibodies on Charged Surfaces by Computer Simulation Based on a United-Residue Model. *Langmuir ACS J. Surf. Colloids* **2003**, *19*, 3472–3478. [[CrossRef](#)]
45. Xie, Y.; Li, Z.; Zhou, J. Hamiltonian replica exchange simulations of glucose oxidase adsorption on charged surfaces. *Phys. Chem. Chem. Phys.* **2018**, *20*, 14587–14596. [[CrossRef](#)] [[PubMed](#)]
46. Yu, G.B.; Zhou, J. Understanding the curvature effect of silica nanoparticles on lysozyme adsorption orientation and conformation: A mesoscopic coarse-grained simulation study. *Phys. Chem. Chem. Phys.* **2016**, *18*, 23500–23507. [[CrossRef](#)] [[PubMed](#)]
47. Carlsson, F.; Hyltner, E.; Arnebrant, T.; Malmsten, M.; Linse, P. Lysozyme Adsorption to Charged Surfaces. A Monte Carlo Study. *J. Phys. Chem. B* **2004**, *108*, 9871–9881. [[CrossRef](#)]
48. Mücksch, C.; Urbassek, H.M. Molecular Dynamics Simulation of Free and Forced BSA Adsorption on a Hydrophobic Graphite Surface. *Langmuir ACS J. Surf. Colloids* **2011**, *27*, 12938–12943. [[CrossRef](#)]
49. Ganazzoli, F.; Raffaini, G. Computer simulation of polypeptide adsorption on model biomaterials. *Phys. Chem. Chem. Phys.* **2005**, *7*, 3651–3663. [[CrossRef](#)]
50. Thingholm, T.; Jørgensen, T.J.; Jensen, O.N.; Larsen, M.R. Highly selective enrichment of phosphorylated peptides using titanium dioxide. *Nat. Protoc.* **2006**, *1*, 1929–1935. [[CrossRef](#)]
51. Dimer, F.; Petzold, M.; Hubbuch, J. Effects of ionic strength and mobile phase pH on the binding orientation of lysozyme on different ion-exchange adsorbents. *J. Chromatogr. A* **2008**, *1194*, 11–21. [[CrossRef](#)] [[PubMed](#)]
52. Tu, X.; Manohar, S.; Jagota, A.; Zheng, M. DNA sequence motifs for structure-specific recognition and separation of carbon nanotubes. *Nature* **2009**, *460*, 250–253. [[CrossRef](#)] [[PubMed](#)]
53. Koga, M.; Kurebayashi, S.; Murai, J.; Saito, H.; Miyazaki, A. Degree of discrepancy between HbA_{1c} and glycemia in variant hemoglobin is smaller when HbA_{1c} is measured by new-type Arkray HPLC compared with old-type HPLC. *Clin. Biochem.* **2014**, *47*, 123–125. [[CrossRef](#)] [[PubMed](#)]
54. Toumadje, A.; Alcorn, S.W.; Johnson, W.C. Extending CD spectra of proteins to 168 nm improves the analysis for secondary structures. *Anal. Biochem.* **1992**, *200*, 321–331. [[CrossRef](#)]
55. Roth, C.M.; Lenhoff, A.M. Electrostatic and vanderwaals contributions to protein adsorption—Computation of equilibrium constants. *Langmuir ACS J. Surf. Colloids* **1993**, *9*, 962–972. [[CrossRef](#)]
56. Dyr, J.E.; Suttner, J. Separation used for purification of recombinant proteins. *J. Chromatogr. B Biomed. Sci. Appl.* **1997**, *699*, 383–401. [[CrossRef](#)]

57. Walkey, C.D.; Chan, W.C.W. Understanding and controlling the interaction of nanomaterials with proteins in a physiological environment. *Chem. Soc. Rev.* **2012**, *41*, 2780–2799. [[CrossRef](#)]
58. Nawrocki, J.; Dunlap, C.; McCormick, A.; Carr, P.J.J. Part I. Chromatography using ultra-stable metal oxide-based stationary phases for HPLC. *J. Chromatogr. A* **2004**, *1028*, 1–30. [[CrossRef](#)]
59. Nawrocki, J.; Dunlap, C.; Li, J.; Zhao, J.; McNeff, C.; McCormick, A.; Carr, P.J.J. Part II. Chromatography using ultra-stable metal oxide-based stationary phases for HPLC. *J. Chromatogr. A* **2004**, *1028*, 31–62. [[CrossRef](#)]
60. Tsai, P.; Wu, C.-T.; Lee, C.S. Electrokinetic studies of inorganic coated capillaries. *J. Chromatogr. B Biomed. Sci. Appl.* **1994**, *657*, 285–290. [[CrossRef](#)]
61. Engholm-Keller, K.; Larsen, M.R. Titanium dioxide as chemo-affinity chromatographic sorbent of biomolecular compounds—Applications in acidic modification-specific proteomics. *J. Proteom.* **2011**, *75*, 317–328. [[CrossRef](#)] [[PubMed](#)]
62. Kawahara, M.; Nakamura, H.; Nakajima, T. Titania and zirconia: Possible new ceramic microparticulates for high-performance liquid chromatography. *J. Chromatogr. A* **1990**, *515*, 149–158. [[CrossRef](#)]
63. Winkler, J.; Marmé, S. Titania as a sorbent in normal-phase liquid chromatography. *J. Chromatogr. A* **2000**, *888*, 51–62. [[CrossRef](#)]
64. Mazanek, M.; Mituloviae, G.; Herzog, F.; Stingl, C.; Hutchins, J.R.A.; Peters, J.-M.; Mechtler, K. Titanium dioxide as a chemo-affinity solid phase in offline phosphopeptide chromatography prior to HPLC-MS/MS analysis. *Nat. Protoc.* **2006**, *2*, 1059–1069. [[CrossRef](#)] [[PubMed](#)]
65. Wijeratne, A.B.; Wijesundera, D.N.; Paulose, M.; Ahiabu, I.B.; Chu, W.-K.; Varghese, O.K.; Greis, K.D. Phos-phopeptide Separation Using Radially Aligned Titania Nanotubes on Titanium Wire. *ACS Appl. Mater. Interfaces* **2015**, *7*, 11155–11164. [[CrossRef](#)]
66. An, R.; Zhuang, W.; Yang, Z.; Lu, X.; Zhu, J.; Wang, Y.; Dong, Y.; Wu, N. Protein adsorptive behavior on meso-porous titanium dioxide determined by geometrical topography. *Chem. Eng. Sci.* **2014**, *117*, 146–155. [[CrossRef](#)]
67. Huangfu, C.; Dong, Y.; Ji, X.; Wu, N.; Lu, X. Mechanistic Study of Protein Adsorption on Mesoporous TiO₂ in Aqueous Buffer Solutions. *Langmuir ACS J. Surf. Colloids* **2019**, *35*, 11037–11047. [[CrossRef](#)]
68. Kupcik, R.; Macak, J.M.; Rehulkova, H.; Sopha, H.; Fabrik, I.; Anitha, V.C.; Klimentova, J.; Murasova, P.; Bilkova, Z.; Rehulka, P. Amorphous TiO₂ Nanotubes as a Platform for Highly Selective Phosphopeptide Enrichment. *ACS Omega* **2019**, *4*, 12156–12166. [[CrossRef](#)]
69. Shen, Q.; Cheung, H.-Y. TiO₂/SiO₂ Core-Shell Composite-Based Sample Preparation Method for Selective Extraction of Phospholipids from Shrimp Waste Followed by Hydrophilic Interaction Chromatography Coupled with Quadrupole Time-of-Flight/Mass Spectrometry Analysis. *J. Agric. Food Chem.* **2014**, *62*, 8944–8951. [[CrossRef](#)]
70. Dong, Y.; Laaksonen, A.; Gong, M.; An, R.; Ji, X. Selective Separation of Highly Similar Proteins on Ionic Liquid-Loaded Mesoporous TiO₂. *Langmuir ACS J. Surf. Colloids* **2022**, *38*, 3202–3211. [[CrossRef](#)]
71. Binnig, G.; Quate, C.F.; Gerber, C.J.P. Atomic force microscope. *Phys. Rev. Lett.* **1986**, *56*, 930. [[CrossRef](#)] [[PubMed](#)]
72. Willemsen, O.H.; Snel, M.M.; Cambi, A.; Greve, J.; De Groot, B.G.; Figdor, C.G. Biomolecular Interactions Measured by Atomic Force Microscopy. *Biophys. J.* **2000**, *79*, 3267–3281. [[CrossRef](#)]
73. Cacciafesta, P.; Humphris, A.D.L.; Jandt, K.D.; Miles, M.J. Human Plasma Fibrinogen Adsorption on Ultraflat Titanium Oxide Surfaces Studied with Atomic Force Microscopy. *Langmuir ACS J. Surf. Colloids* **2000**, *16*, 8167–8175. [[CrossRef](#)]
74. Sousa, S.R.; Brás, M.M.; Moradas-Ferreira, P.; Barbosa, M.A. Dynamics of Fibronectin Adsorption on TiO₂ Surfaces. *Langmuir ACS J. Surf. Colloids* **2007**, *23*, 7046–7054. [[CrossRef](#)] [[PubMed](#)]
75. Li, G.; Nandgaonkar, A.G.; Wang, Q.; Zhang, J.; Krause, W.E.; Wei, Q.; Lucia, L. Laccase-immobilized bacterial cellulose/TiO₂ functionalized composite membranes: Evaluation for photo- and bio-catalytic dye degradation. *J. Membr. Sci.* **2017**, *525*, 89–98. [[CrossRef](#)]
76. Scholl, Z.N.; Marszalek, P.E. AFM-Based Single-Molecule Force Spectroscopy of Proteins. In *Nanoscale Imaging*; Humana Press: New York, NY, USA, 2018; pp. 35–47. [[CrossRef](#)]
77. Petrosyan, R.; Narayan, A.; Woodside, M.T. Single-Molecule Force Spectroscopy of Protein Folding. *J. Mol. Biol.* **2021**, *433*, 167207. [[CrossRef](#)] [[PubMed](#)]
78. Verdorfer, T.; Bernardi, R.C.; Meinhold, A.; Ott, W.; Luthey-Schulten, Z.; Nash, M.A.; Gaub, H.E. Combining in Vitro and in Silico Single-Molecule Force Spectroscopy to Characterize and Tune Cellulosomal Scaffoldin Mechanics. *J. Am. Chem. Soc.* **2017**, *139*, 17841–17852. [[CrossRef](#)]
79. Ma, L.; Cai, Y.; Li, Y.; Jiao, J.; Wu, Z.; O’Shaughnessy, B.; De Camilli, P.; Karatekin, E.; Zhang, Y. Single-molecule force spectroscopy of protein-membrane interactions. *eLife* **2017**, *6*, e30493. [[CrossRef](#)]
80. Hoffmann, T.; Dougan, L. Single molecule force spectroscopy using polyproteins. *Chem. Soc. Rev.* **2012**, *41*, 4781–4796. [[CrossRef](#)]
81. Huang, W.; Wu, X.; Gao, X.; Yu, Y.; Lei, H.; Zhu, Z.; Shi, Y.; Chen, Y.; Qin, M.; Wang, W.; et al. Maleimide–thiol adducts stabilized through stretching. *Nat. Chem.* **2019**, *11*, 310–319. [[CrossRef](#)]
82. Ganbaatar, N.; Imai, K.; Yano, T.-A.; Hara, M. Surface force analysis of glycine adsorption on different crystal surfaces of titanium dioxide (TiO₂). *Nano Converg.* **2017**, *4*, 38. [[CrossRef](#)] [[PubMed](#)]
83. Leader, A.; Mandler, D.; Reches, M. The role of hydrophobic, aromatic and electrostatic interactions between amino acid residues and a titanium dioxide surface. *Phys. Chem. Chem. Phys.* **2018**, *20*, 29811–29816. [[CrossRef](#)] [[PubMed](#)]
84. Vergaro, V.; Carlucci, C.; Cascione, M.; Lorusso, C.; Conciauro, F.; Scremin, B.F.; Congedo, P.M.; Cannazza, G.; Citti, C.; Ciccarella, G.J.N. Nanotechnology, Interaction between human serum albumin and different anatase TiO₂ nanoparticles: A nano-bio interface study. *Nanomater. Nanotechnol.* **2015**, *5*, 30. [[CrossRef](#)]

85. Dong, Y.; An, R.; Zhao, S.; Cao, W.; Huang, L.; Zhuang, W.; Lu, L.; Lu, X. Molecular Interactions of Protein with TiO₂ by the AFM-Measured Adhesion Force. *Langmuir ACS J. Surf. Colloids* **2017**, *33*, 11626–11634. [[CrossRef](#)]
86. Dong, Y.; Ji, X.; Laaksonen, A.; Cao, W.; He, H.; Lu, X. Excellent Protein Immobilization and Stability on Heterogeneous C-TiO₂ Hybrid Nanostructures: A Single Protein AFM Study. *Langmuir ACS J. Surf. Colloids* **2020**, *36*, 9323–9332. [[CrossRef](#)]
87. Ventura, S.P.M.; Silva, F.A.E.; Quental, M.V.; Mondal, D.; Freire, M.G.; Coutinho, J.A.P. Ionic-Liquid-Mediated Extraction and Separation Processes for Bioactive Compounds: Past, Present, and Future Trends. *Chem. Rev.* **2017**, *117*, 6984–7052. [[CrossRef](#)]
88. Freire, M.G.; Cláudio, A.F.M.; Araújo, J.M.M.; Coutinho, J.A.P.; Marrucho, I.M.; Lopes, J.N.C.; Rebelo, L.P.N. Aqueous biphasic systems: A boost brought about by using ionic liquids. *Chem. Soc. Rev.* **2012**, *41*, 4966–4995. [[CrossRef](#)]
89. Dong, Y.; Laaksonen, A.; Huo, F.; Gao, Q.; Ji, X. Hydrated Ionic Liquids Boost the Trace Detection Capacity of Proteins on TiO₂ Support. *Langmuir ACS J. Surf. Colloids* **2021**, *37*, 5012–5021. [[CrossRef](#)]
90. Qi, D.; Lu, L.; Wang, L.; Zhang, J. Improved SERS Sensitivity on Plasmon-Free TiO₂ Photonic Microarray by Enhancing Light-Matter Coupling. *J. Am. Chem. Soc.* **2014**, *136*, 9886–9889. [[CrossRef](#)] [[PubMed](#)]
91. Han, X.X.; Ji, W.; Zhao, B.; Ozaki, Y. Semiconductor-enhanced Raman scattering: Active nanomaterials and applications. *Nanoscale* **2017**, *9*, 4847–4861. [[CrossRef](#)] [[PubMed](#)]
92. Alessandri, I.; Lombardi, J.R. Enhanced Raman Scattering with Dielectrics. *Chem. Rev.* **2016**, *116*, 14921–14981. [[CrossRef](#)] [[PubMed](#)]
93. Cong, S.; Liu, X.; Jiang, Y.; Zhang, W.; Zhao, Z. Surface Enhanced Raman Scattering Revealed by Interfacial Charge-Transfer Transitions. *Innovation* **2020**, *1*, 100051. [[CrossRef](#)] [[PubMed](#)]
94. Yilmaz, M.; Babur, E.; Ozdemir, M.; Giesecking, R.L.; Dede, Y.; Tamer, U.; Schatz, G.C.; Facchetti, A.; Usta, H.; Demirel, G. Nanostructured organic semiconductor films for molecular detection with surface-enhanced Raman spectroscopy. *Nat. Mater.* **2017**, *16*, 918–924. [[CrossRef](#)] [[PubMed](#)]
95. Shoute, L.C.T.; Loppnow, G.R. Excited-state dynamics of alizarin-sensitized TiO₂ nanoparticles from resonance Raman spectroscopy. *J. Chem. Phys.* **2002**, *117*, 842–850. [[CrossRef](#)]
96. Yang, L.; Jiang, X.; Ruan, W.; Zhao, B.; Xu, W.; Lombardi, J.R. Observation of Enhanced Raman Scattering for Molecules Adsorbed on TiO₂ Nanoparticles: Charge-Transfer Contribution. *J. Phys. Chem. C* **2008**, *112*, 20095–20098. [[CrossRef](#)]
97. Yang, L.; Gong, M.; Jiang, X.; Yin, D.; Qin, X.; Zhao, B.; Ruan, W. Investigation on SERS of different phase structure TiO₂ nanoparticles. *J. Raman Spectrosc.* **2015**, *46*, 287–292. [[CrossRef](#)]
98. Yang, L.; Qin, X.; Jiang, X.; Gong, M.; Yin, D.; Zhang, Y.; Zhao, B. SERS investigation of ciprofloxacin drug molecules on TiO₂ nanoparticles. *Phys. Chem. Chem. Phys.* **2015**, *17*, 17809–17815. [[CrossRef](#)]
99. Chen, L.; Cai, L.; Ruan, W.; Zhao, B. Surface-Enhanced Raman Spectroscopy: Protein Application. *Encycl. Anal. Chem.* **2018**, 1–25. [[CrossRef](#)]
100. Li, X.; Chen, G.; Yang, L.; Jin, Z.; Liu, J. Multifunctional Au-Coated TiO₂ Nanotube Arrays as Recyclable SERS Substrates for Multifold Organic Pollutants Detection. *Adv. Funct. Mater.* **2010**, *20*, 2815–2824. [[CrossRef](#)]
101. Ling, Y.; Zhuo, Y.; Huang, L.; Mao, D. Using Ag-embedded TiO₂ nanotubes array as recyclable SERS substrate. *Appl. Surf. Sci.* **2016**, *388*, 169–173. [[CrossRef](#)]
102. Roguska, A.; Kudelski, A.; Pisarek, M.; Lewandowska, M.; Dolata, M.; Janik-Czachor, M. Raman investigations of TiO₂ nanotube substrates covered with thin Ag or Cu deposits. *J. Raman Spectrosc.* **2009**, *40*, 1652–1656. [[CrossRef](#)]
103. Zhou, L.; Zhou, J.; Lai, W.; Yang, X.; Meng, J.; Su, L.; Gu, C.; Jiang, T.; Pun, E.Y.B.; Shao, L.; et al. Irreversible accumulated SERS behavior of the molecule-linked silver and silver-doped titanium dioxide hybrid system. *Nat. Commun.* **2020**, *11*, 1785. [[CrossRef](#)] [[PubMed](#)]
104. Han, X.X.; Koehler, C.; Kozuch, J.; Kuhlmann, U.; Paasche, L.; Sivanesan, A.; Weidinger, I.M.; Hildebrandt, P. Potential-Dependent Surface-Enhanced Resonance Raman Spectroscopy at Nanostructured TiO₂: A Case Study on Cytochrome b(5). *Small* **2013**, *9*, 4175–4181. [[CrossRef](#)] [[PubMed](#)]
105. Alessandri, I. Enhancing Raman Scattering without Plasmons: Unprecedented Sensitivity Achieved by TiO₂ Shell-Based Resonators. *J. Am. Chem. Soc.* **2013**, *135*, 5541–5544. [[CrossRef](#)]
106. Roy, P.; Berger, S.; Schmuki, P. TiO₂ Nanotubes: Synthesis and Applications. *Angew. Chem. Int. Ed.* **2011**, *50*, 2904–2939. [[CrossRef](#)] [[PubMed](#)]
107. Lee, K.; Mazare, A.; Schmuki, P. One-Dimensional Titanium Dioxide Nanomaterials: Nanotubes. *Chem. Rev.* **2014**, *114*, 9385–9454. [[CrossRef](#)] [[PubMed](#)]
108. Öner, I.H.; Querebillo, C.J.; David, C.; Gernert, U.; Walter, C.; Driess, M.; Leimkühler, S.; Ly, K.H.; Weidinger, I.M.; Oener, H.I. High Electromagnetic Field Enhancement of TiO₂ Nanotube Electrodes. *Angew. Chem. Int. Ed.* **2018**, *57*, 7225–7229. [[CrossRef](#)]
109. Liu, L.; Pan, F.; Liu, C.; Huang, L.; Li, W.; Lu, X. TiO₂ Nanofoam–Nanotube Array for Surface-Enhanced Raman Scattering. *ACS Appl. Nano Mater.* **2018**, *1*, 6563–6566. [[CrossRef](#)]
110. Dong, Y.; Ji, X.; Laaksonen, A.; Cao, W.; An, R.; Lu, L.; Lu, X. Determination of the small amount of proteins inter-acting with TiO₂ nanotubes by AFM-measurement. *Biomaterials* **2019**, *192*, 368–376. [[CrossRef](#)]
111. Shaik, U.P.; Hamad, S.; Mohiddon, A.; Soma, V.R.; Krishna, M.G. Morphologically manipulated Ag/ZnO nanostructures as surface enhanced Raman scattering probes for explosives detection. *J. Appl. Phys.* **2016**, *119*, 093103. [[CrossRef](#)]
112. Qian, L.H.; Yan, X.Q.; Fujita, T.; Inoue, A.; Chen, M. Surface enhanced Raman scattering of nanoporous gold: Smaller pore sizes stronger enhancements. *Appl. Phys. Lett.* **2007**, *90*, 153120. [[CrossRef](#)]

113. Dong, Y.; Wu, N.; Ji, X.; Laaksonen, A.; Lu, X.; Zhang, S. Excellent Trace Detection of Proteins on TiO₂ Nanotube Substrates through Novel Topography Optimization. *J. Phys. Chem. C* **2020**, *124*, 27790–27800. [[CrossRef](#)]
114. Ding, Q.; Wang, J.; Chen, X.; Liu, H.; Li, Q.; Wang, Y.; Yang, S. Quantitative and Sensitive SERS Platform with Analyte Enrichment and Filtration Function. *Nano Lett.* **2020**, *20*, 7304–7312. [[CrossRef](#)] [[PubMed](#)]
115. Agafilushkina, S.N.; Zulkovskaja, O.; Dyakov, S.A.; Weber, K.; Sivakov, V.; Popp, J.; Cialla-May, D.; Osminkina, L.A. Raman Signal Enhancement Tunable by Gold-Covered Porous Silicon Films with Different Morphology. *Sensors* **2020**, *20*, 5634. [[CrossRef](#)] [[PubMed](#)]
116. Wang, G.; Yi, R.; Zhai, X.; Bian, R.; Gao, Y.; Cai, D.; Liu, J.; Huang, X.; Lu, G.; Li, H.; et al. A flexible SERS-active film for studying the effect of non-metallic nanostructures on Raman enhancement. *Nanoscale* **2018**, *10*, 16895–16901. [[CrossRef](#)] [[PubMed](#)]
117. Zhang, W.; Tian, Q.; Chen, Z.; Zhao, C.; Chai, H.; Wu, Q.; Li, W.; Chen, X.; Deng, Y.; Song, Y. Arrayed nanopore silver thin films for surface-enhanced Raman scattering. *RSC Adv.* **2020**, *10*, 23908–23915. [[CrossRef](#)]
118. Hurst, S.J.; Fry, H.C.; Gosztola, D.J.; Rajh, T. Utilizing Chemical Raman Enhancement: A Route for Metal Oxide Support-Based Biodetection. *J. Phys. Chem. C* **2011**, *115*, 620–630. [[CrossRef](#)]
119. Jiang, X.; Xu, L.; Ji, W.; Wang, W.; Du, J.; Yang, L.; Song, W.; Han, X.; Zhao, B. One plus one greater than Two: Ultrasensitive Surface-Enhanced Raman Scattering by TiO₂/ZnO Heterojunctions Based on Electron-Hole Separation. *Appl. Surf. Sci.* **2022**, *584*, 152609. [[CrossRef](#)]
120. Das, S.; Saxena, K.; Goswami, L.P.; Gayathri, J.; Mehta, D.S. Mesoporous Ag–TiO₂ based nanocage like structure as sensitive and recyclable low-cost SERS substrate for biosensing applications. *Opt. Mater.* **2022**, *125*, 111994. [[CrossRef](#)]
121. Xu, W.; Mao, N.; Zhang, J. Graphene: A Platform for Surface-Enhanced Raman Spectroscopy. *Small* **2013**, *9*, 1206–1224. [[CrossRef](#)]
122. Nordness, O.; Brennecke, J.F. Ion Dissociation in Ionic Liquids and Ionic Liquid Solutions. *Chem. Rev.* **2020**, *120*, 12873–12902. [[CrossRef](#)] [[PubMed](#)]
123. Ma, C.; Laaksonen, A.; Liu, C.; Lu, X.; Ji, X. The peculiar effect of water on ionic liquids and deep eutectic solvents. *Chem. Soc. Rev.* **2018**, *47*, 8685–8720. [[CrossRef](#)] [[PubMed](#)]
124. Peng, C.; Liu, J.; Zhou, J. Molecular Simulations of Cytochrome c Adsorption on a Bare Gold Surface: Insights for the Hindrance of Electron Transfer. *J. Phys. Chem. C* **2015**, *119*, 20773–20781. [[CrossRef](#)]
125. Quan, X.; Liu, J.; Zhou, J. Multiscale modeling and simulations of protein adsorption: Progresses and perspectives. *Curr. Opin. Colloid Interface Sci.* **2018**, *41*, 74–85. [[CrossRef](#)]
126. Guo, C.; Wu, C.; Chen, M.; Zheng, T.; Chen, N.; Cummings, P.T. Molecular modeling of fibronectin adsorption on topographically nanostructured rutile (110) surfaces. *Appl. Surf. Sci.* **2016**, *384*, 36–44. [[CrossRef](#)]
127. Kang, Y.; Li, X.; Tu, Y.; Wang, Q.; Ågren, H. On the Mechanism of Protein Adsorption onto Hydroxylated and Non-hydroxylated TiO₂ Surfaces. *J. Phys. Chem. C* **2010**, *114*, 14496–14502. [[CrossRef](#)]
128. Zheng, T.; Zhang, Y.; Wu, C.; Zhou, L.; Cummings, P.T. Molecular investigations of tripeptide adsorption onto TiO₂ surfaces: Synergetic effects of surface nanostructure, hydroxylation and bioactive ions. *Appl. Surf. Sci.* **2020**, *512*, 145713. [[CrossRef](#)]
129. Wu, C.; Chen, M.; Xing, C. Molecular Understanding of Conformational Dynamics of a Fibronectin Module on Rutile (110) Surface. *Langmuir ACS J. Surf. Colloids* **2010**, *26*, 15972–15981. [[CrossRef](#)] [[PubMed](#)]
130. Wu, C.; Skelton, A.A.; Chen, M.; Vlček, L.; Cummings, P.T. Modeling the Interaction between Integrin-Binding Peptide (RGD) and Rutile Surface: The Effect of Cation Mediation on Asp Adsorption. *Langmuir ACS J. Surf. Colloids* **2012**, *28*, 2799–2811. [[CrossRef](#)]
131. Yang, C.; Peng, C.; Zhao, D.; Liao, C.; Zhou, J.; Lu, X. Molecular simulations of myoglobin adsorbed on rutile (1 1 0) and (0 0 1) surfaces. *Fluid Phase Equilib.* **2014**, *362*, 349–354. [[CrossRef](#)]
132. Wu, X.; Hao, P.; He, F.; Yao, Z.; Zhang, X. Molecular dynamics simulations of BSA absorptions on pure and for-mate-contaminated rutile (110) surface. *Appl. Surf. Sci.* **2020**, *533*, 147574. [[CrossRef](#)]
133. Wu, X.; Wang, C.; Hao, P.; He, F.; Yao, Z.; Zhang, X. Adsorption properties of albumin and fibrinogen on hydrophilic/hydrophobic TiO₂ surfaces: A molecular dynamics study. *Colloids Surf. B Biointerfaces* **2021**, *207*, 111994. [[CrossRef](#)] [[PubMed](#)]
134. Zhang, Z.L.; Sheng, S.X.; Wang, R.M.; Sun, M.T. Tip-Enhanced Raman Spectroscopy. *Anal. Chem.* **2016**, *88*, 9328–9346. [[CrossRef](#)] [[PubMed](#)]
135. Verma, P. Tip-Enhanced Raman Spectroscopy: Technique and Recent Advances. *Chem. Rev.* **2017**, *117*, 6447–6466. [[CrossRef](#)]
136. Kushiro, K.; Lee, C.H.; Takai, M. Simultaneous characterization of protein-material and cell-protein interactions using dynamic QCM-D analysis on SAM surfaces. *Biomater. Sci.* **2016**, *6*, 989–997. [[CrossRef](#)] [[PubMed](#)]
137. Tan, S.W.; Sut, T.N.; Jeon, W.-Y.; Yoon, B.K.; Jackman, J.A. On/off switching of lipid bicelle adsorption on titanium oxide controlled by sub-monolayer molecular surface functionalization. *Appl. Mater. Today* **2022**, *27*, 101444. [[CrossRef](#)]
138. Fabre, H.; Mercier, D.; Galtayries, A.; Portet, D.; Delorme, N.; Bardeau, J.-F. Impact of hydrophilic and hydrophobic functionalization of flat TiO₂/Ti surfaces on proteins adsorption. *Appl. Surf. Sci.* **2018**, *432*, 15–21. [[CrossRef](#)]
139. Chen, X.; Ferrigno, R.; Yang, A.J.; Whitesides, G.M. Redox Properties of Cytochrome c Adsorbed on Self-Assembled Monolayers: A Probe for Protein Conformation and Orientation. *Langmuir ACS J. Surf. Colloids* **2002**, *18*, 7009–7015. [[CrossRef](#)]
140. Tollin, G.; Salamon, Z.; Hruby, V.J. Techniques: Plasmon-waveguide resonance (PWR) spectroscopy as a tool to study ligand-GPCR interactions. *Trends Pharmacol. Sci.* **2003**, *24*, 655–659. [[CrossRef](#)]

141. Kovacs, N.; Patko, D.; Orgovan, N.; Kurunczi, S.; Ramsden, J.J.; Vonderviszt, F.; Horvath, R. Optical Anisotropy of Flagellin Layers: In Situ and Label-Free Measurement of Adsorbed Protein Orientation Using OWLS. *Anal. Chem.* **2013**, *85*, 5382–5389. [[CrossRef](#)]
142. Patko, D.; Cottier, K.; Hamori, A.; Horvath, R. Single beam grating coupled interferometry: High resolution miniaturized label-free sensor for plate based parallel screening. *Opt. Express* **2012**, *20*, 23162–23173. [[CrossRef](#)] [[PubMed](#)]